

Wind-generated long wave climate in the Tvärminne area

Kimmo K. Kahma

Finnish Meteorological Institute, P.O. Box 503, FI-00101 Helsinki, Finland
Corresponding author, kimmo.kahma@kolumbus.fi

(Submitted: December 8, 2021; Accepted: December 31, 2021)

Abstract

Several studies have shown that the wave climate in the archipelago sheltering the Finnish coast varies much within short distances. During the years 2011–2015 The Finnish Transport and Communications Agency (Traficom) financed a wave modelling project to establish navigational rules for ships operating in sheltered waters. The data of that project is used here to produce a map of the area surrounding the Tvärminne Zoological Station about the significant wave height of long waves that is exceeded 10 % of the time when the sea is not ice covered. The map provides useful information that can be used as a proxy for the current velocities near the bottom.

Keywords: Wave model; Gulf of Finland; Tvärminne; wave climate; refraction

1 Introduction

The Gulf of Finland is in many respects a unique environment. This applies among other features to the wind-generated waves, which subsequently affect several other aspects of the marine environment. The elongated shape of the gulf modifies the waves in important ways. First of all, the significant wave height decreases from the mouth towards the end of the gulf (Tuomi *et al.*, 2011), and climatologically, the wave height has fallen considerably already before Tvärminne. Fig. 1 shows the significant wave height that is exceeded 10 % of the time when the sea is not ice covered.

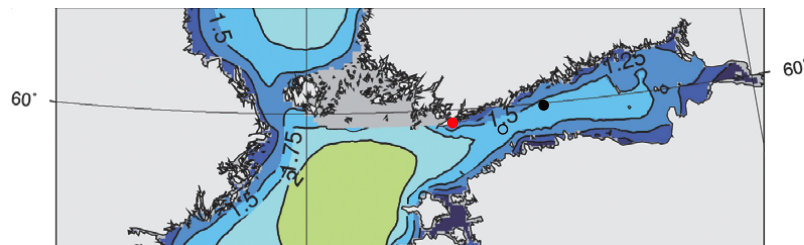


Fig. 1: Significant wave height that is exceeded 10% of the time when the sea is not ice covered. Tvärminne is shown (red bullet) as well as the wave measuring sites Porkkala (open circle), and Helsinki (bullet). Modified from Tuomi *et al.* (2011)

Secondly, when the wind is in the direction of the gulf, the waves grow less rapidly with fetch than in the case when the wind direction is orthogonal to the shore (Kahma and

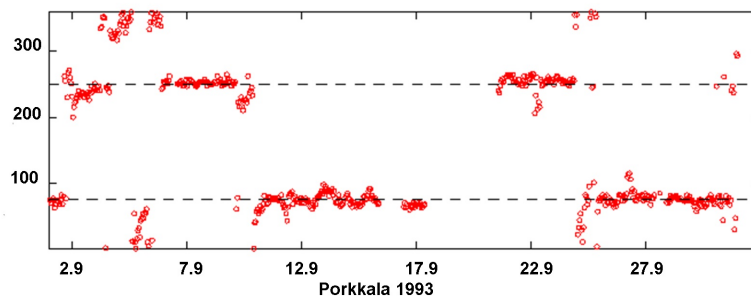


Fig. 2: Time series showing the steering of the wave directions in the Gulf of Finland. The dashed lines indicate the orientation of the axis of the gulf. Modified from *Pettersson et al.* (2010)

Pettersson, 1994). Thirdly, the wave spectrum does not have the shape it has when waves grow in ideal conditions (*Pettersson*, 2004). Finally, when the wind is not in the direction of the gulf axis, the dominant wave direction differs from the wind direction (*Pettersson et al.*, 2010). Fig. 2 shows that in most cases the dominant waves come either from 240° or from 90° . Fig. 3 shows that this is not because the wind predominantly comes from these directions. Only when the wind is orthogonal to the shore do the dominant waves follow the wind direction.

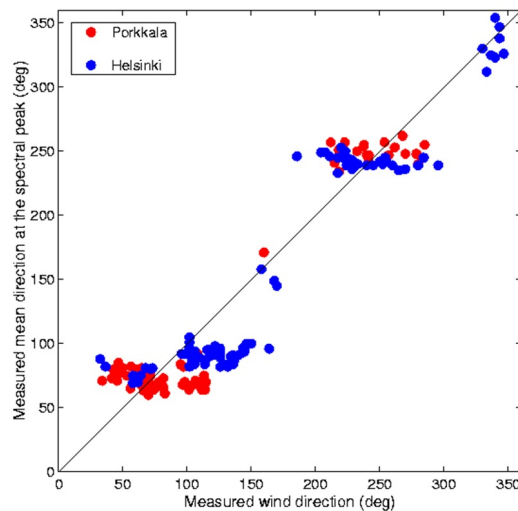


Fig. 3: The mean direction at the spectral peak versus wind direction. From *Pettersson* (2004)

This curious phenomenon can be explained by the weak nonlinear wave-wave interactions. These resist the change of the wave direction when the wind turns, as shown by *van Vledder* (1990). *Pettersson* (2004) pointed out that the situation is analogous when the wind direction is not orthogonal to the shore of a narrow gulf, and suggested the following mechanism for the steering of the waves: When waves grow from the shore the dominant waves initially grow in the wind direction, but these waves eventually run up against the opposite shore of the gulf. Their height is limited by the fetch in the wind direction, and in a steady wind at a fixed distance from the shore the height remains constant regardless of how far along the gulf they are. Those waves that grow in the direction of the gulf

lose a significant part of their energy to the dominant waves via nonlinear interactions, but not all the energy they get from the wind. Thus, as they slowly grow along the direction of the gulf, their growth will not terminate at the shoreline of the gulf. The waves in the gulf direction keep growing, and eventually will become larger than the waves in the wind direction. At that point they become the dominant waves that capture the energy via nonlinear interactions from the waves in the wind direction.

Most of the coastline of Finland is sheltered by an archipelago several kilometers deep consisting of thousands of islands of various sizes. The smallest are tiny rocks that are not even visible in maps on the scale of Fig. 4. When the waves propagate into this archipelago they are modified by refraction, by diffraction, and by the sheltering of the islands. The properties of the waves have been measured and modelled in several places along the Finnish coast. The first studies were in the archipelago of Pyhämaa (*Kahma*, 1979). Further studies have been carried out off Rauma, Raahelampi, Mäntyluoto, Vuosaari, Utö (*Tuomi et al.*, 2014), and, most recently, in the archipelago of Helsinki where measurements were made at 21 points (*Kahma et al.*, 2016; *Björkqvist et al.*, 2017). These studies show that the wave conditions vary considerably within short distances, even at the same distance from the mainland. Even in ideal conditions, when the open sea wave spectrum has a relatively simple structure, the wave spectrum in the archipelago is more variable. The spectrum may form a two-peak structure where neither of the peaks are swell waves (*Kahma*, 1981), or a band-passed white spectrum (*Björkqvist et al.*, 2017). Deep in the archipelago, where the open sea waves have almost completely died out, the spectrum again recovers the simple one-peak form but now at a new, much smaller significant wave height and modal period. For the details of this transformation see, e.g., *Björkqvist et al.* (2019).

When we add to these local effects the large-scale effects mentioned above, the result is that the wave climate in two otherwise similar areas of the archipelago will be different in different parts of the Gulf of Finland. And this will apply to all phenomena in the marine environment that are affected by waves, be they purely oceanographical or applications such as seakeeping.

During the years 2011–2015 the Finnish Transport and Communications Agency (Traficom) financed a wave modelling project to establish navigational rules for ships operating in sheltered waters, but the report has not been published. Because neither measurements nor wave model studies have been published for the area surrounding the Tvärminne Zoological Station, we present here a description of the methods and a map for this area based on the data produced for the unpublished report *Kahma et al.* (2015).

2 Methods: The wave models

Two wave models as well as measured data from the Northern Baltic proper and the Gulf of Finland were used to generate a map of the significant wave height that is exceeded 10 % of the time when the sea is not ice covered. Significant wave height H_s is here defined in the usual way as $H_s = 4\sqrt{m_0}$, where m_0 is the zeroth moment of the wave spectrum. The open sea wave climatology shown in Fig. 1 was modelled by a third-generation WAM

wave model (*Komen et al.*, 1994). The implementation of the 22 km grid size model and calculations are described in *Tuomi et al.* (2011).

A WAM version with a grid size of only 240 m was used to give an overview of the total wave height in the archipelago in representative conditions. The computational resources at the time of the project did not allow the WAM model to be calculated with the required 20 m resolution over the whole Finnish coast.

The detailed map was therefore calculated by a refraction model, in which the source terms were assumed to be zero. The Monte-Carlo method proposed by *Bouws and Battjes* (1982) was used. A more detailed description of the refraction model and the bathymetry is given in *Kahma et al.* (2022, in preparation). Here we will discuss only those aspects of the refraction model that are relevant for the interpretation of the results.

For seakeeping purposes, the height of long waves is more relevant than the total wave height. Therefore, the significant height of waves longer than 5 seconds was chosen for the detailed map. We define the variance of long waves as

$$m_c = \int_{-\pi}^{\pi} \int_0^{\omega_c} \underline{\mathbf{S}}(\omega, \theta) d\omega d\theta, \quad (1)$$

where $\underline{\mathbf{S}}$ is the wave spectrum, ω the angular frequency and θ the direction. The significant wave height of waves that are longer than the period $T_c = 2\pi/\omega_c$ is defined as $4\sqrt{m_c}$.

For the refraction model calculations, the coast of Finland was divided into 53 segments small enough that the wave climate in the adjoining open sea area could be assumed to be constant within a segment. The length of a segment was typically *ca.* 10 km (roughly, the diameter of the red dot in Fig. 1). Within this distance the change in the climatological values of significant wave height and direction is clearly less than the uncertainty of the modelling. The Tvärminne region shown in Fig. 4 comprises two such segments.

The refraction model was used within each segment to calculate a large number of wave rays starting at different points in the open sea part of the segment. A ray was terminated when it encountered an island or the mainland. Rays were calculated for all relevant periods $T = 2\pi/\omega$ and initial open sea directions θ . Within the accuracy of the linear wave theory the wave packets conserve their wave action as they move along these rays, provided that the source terms are zero. A description of the wave packet picture for water waves can be found, e.g., in Chapter I of *Komen et al.* (1994).

The packet density in a grid square can then be used to calculate the wave energy E of a sinusoidal wave component as a function of latitude ϕ and longitude λ , at a given period $T = 2\pi/\omega$ and initial open sea direction θ . From the wave energy the refraction coefficient

$$K = \frac{H}{H_0} = \sqrt{\frac{E}{E_0}} \quad (2)$$

was calculated. Here H_0 and E_0 are the open sea values of wave height and wave energy, respectively. At every point (ϕ, λ) the probability of the significant wave height of waves

that are longer than the period $T_c = 2\pi/\omega_c$ could now be estimated by

$$P \left(\int_{-\pi}^{\pi} \int_0^{\omega_c} 16 \underline{\mathbf{S}}(\omega, \theta, t) K^2(\omega, \theta, \phi, \lambda) d\omega d\theta \leq H_1^2(\phi, \lambda) \right). \quad (3)$$

Here P denotes the probability, t is time (covering sufficiently many years), and $\underline{\mathbf{S}}$ is the wave spectrum in the open sea, which is treated here as a random variable. A map of the significant wave height that is exceeded 10 % of the time could in principle be generated by plotting the H_1 that satisfies the condition (3) with probability $P = 0.9$.

The main advantage of the refraction model over WAM is its speed. Even then, full use of Eq. (3) would have required calculations far exceeding the computational resources available for the project, and further approximation was necessary.

The low-frequency part of the wave spectrum below ω_c usually has only a single peak at ω_p and θ_p . While individual rays can be very sensitive to small changes in the initial ω and θ , the density of the wave packets seems to be less sensitive. In the Gulf of Finland the steering of the wave spectrum explained in section 1 has the consequence that only very few direction groups contribute significantly to the integral of Eq. (3). Within such a group Eq. (3) can be approximated by

$$P \left(K(\omega_p, \theta_p, \phi, \lambda) \cdot H_{so}(\omega_p, \theta_p) \leq H_2(\phi, \lambda) \right) = 0.9, \quad (4)$$

where H_{so} satisfies the condition $P(H_{so} \leq H_{so}) = 0.9$, and

$$\underline{H}_{so}(\omega_p(t), \theta_p(t))^2 = \int_{-\pi}^{\pi} \int_0^{\omega_c} 16 \underline{\mathbf{S}}(\omega, \theta, t) d\omega d\theta. \quad (5)$$

Representative small areas were chosen and H_1 was calculated for these. The results were compared with the maps of H_2 . That map of H_2 which in the representative place agreed best with the map of H_1 was then used in the vicinity of that representative place. The final map is a composite of several maps of H_2 .

3 Long wave height map covering the Tvärminne area

The map in Figure 4 shows the significant wave height of long waves that is exceeded 10 % of the time when the sea is not frozen. It is based on an unpublished report by *Kahma et al.* (2015).

The reason for using the long wave height rather than the total wave height in *Kahma et al.* (2015) was that the long wave height is a relevant parameter for seakeeping, as short waves contribute less to the wave-induced motion of a vessel.

Even though T_c was fixed at 5 s, the modal period $T_p = 2\pi/\omega_p$ used in the approximation varied somewhat depending on the wave climate of the area. In the Tvärminne area shown in Figure 4 T_p was 7 s or more.

Practically always the map based on Eq. (3) was smoother and had less detail than the map of the approximation Eq. (4). This means that the map in Figure 4 reveals the

great spatial variability of the wave height in an individual situation. On the other hand, not all the details of Figure 4 are statistically significant climatological features.

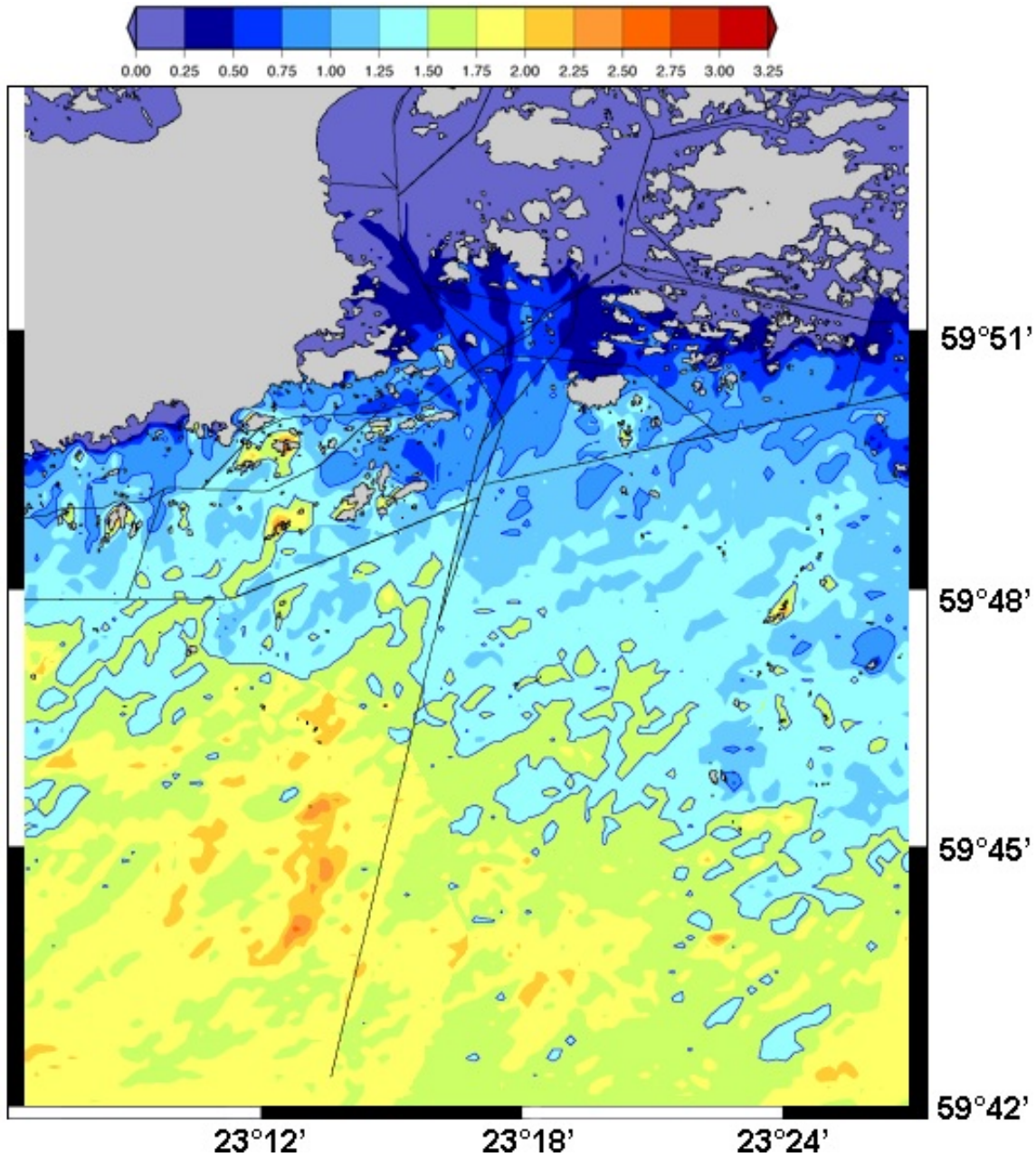


Fig. 4: The significant height (in meters) of long waves that is exceeded 10 % of the time when the sea is not ice covered. The modal period T_p of the long waves was in this area 7 s or more. The lines in the figure are water ways.

4 Applications

While the data was produced for seakeeping purposes, it can be used for other purposes as well. Among them are the wave-induced current velocities near the bottom. According to the linear wave theory, near the bottom the maximum orbital velocity u_{\max} of a

sinusoidal wave of height H is

$$u_{\max} = \frac{H g k}{2 \omega \cosh kh} , \quad (6)$$

where h is the water depth. In the linear wave theory, the wave number $k = 2\pi/L$, the wave length L , the angular frequency ω , and the period T are related through the equation

$$\omega = 2\pi/T = \sqrt{gk \tanh kh} . \quad (7)$$

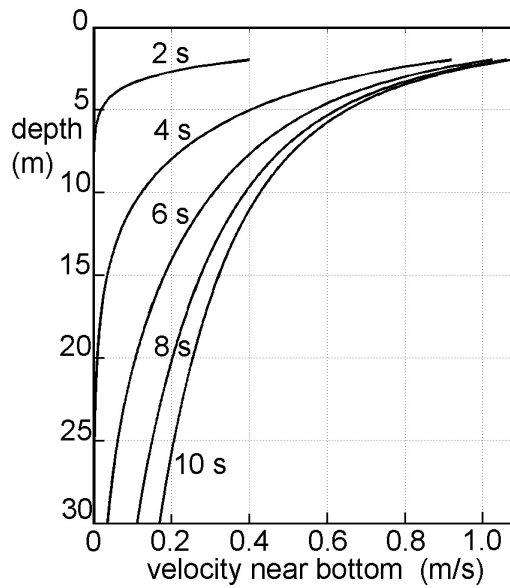


Fig. 5: Maximum orbital velocity near the bottom as a function of wave period when wave height of a sinusoidal wave is 1 m.

Fig. 5 shows that long waves are mainly responsible for the wave-induced currents near the bottom. Fig. 4 thus reveals useful information, in particular when used together with Eq. (6), even though it is far from a comprehensive description of the wave climate, and it is not a substitute for detailed measurements or modelling of wave-induced currents near the bottom.

5 Concluding remarks

The coastline of the Gulf of Finland is protected by an archipelago of thousands of islands of various sizes. The shape of the Gulf itself modifies the wave climate in several ways. These factors combined create a unique wave climate. Detailed modelling of it would be a gigantic task.

This paper uses results of a project in which the wave climate of the entire coastline of Finland was modelled using approximations that made the task possible. While the original motivation was seakeeping, the results are useful for other purposes, e.g., as a proxy for the current velocities near the bottom. Since such values have not yet been

published for the area around Tvärminne Zoological Station, the results are here made public.

When considering the justification for the approximations made in the calculations, it is well to remember that the purpose of the project was to determine the administrative limits of the safety rules for vessels operating in sheltered wave environments. The result is far more representative than either the alternative assumption that the waves in the archipelago are the same as in the open sea, or the approximation that the wave height increases linearly from the shore to the open sea value.

Acknowledgements

The wave modelling project was funded by The Finnish Transport and Communication agency (Traficom), and carried out at the Finnish Meteorological Institute by Kimmo Kahma, Kimmo Tikka, Laura Tuomi, Hannu Jokinen, and Heidi Pettersson. The author thanks Victor Alari and the other referee (anonymous) for their constructive suggestions for improving the manuscript.

References

- Björkqvist, J.-V., H. Pettersson and K. K. Kahma, 2019. The wave spectrum in archipelagos. *Ocean Science*, **15**, 1469–1487. DOI: 10.5194/os-15-1469-2019.
- Björkqvist, J.-V., L. Tuomi, C. Fortelius, H. Pettersson, K. Tikka and K. K. Kahma, 2017. Improved estimates of nearshore wave conditions in the Gulf of Finland. *Journal of Marine Systems*, **171**, 43–53. DOI: 10.1016/j.jmarsys.2016.07.005.
- Bouws, E. and J. A. Battjes, 1982. A Monte Carlo approach to the computation of refraction of water waves. *Journal of Geophysical Research*, **87**, 5718–5722.
- Kahma, K. K., 1979. *On a two-peak structure in steady-state fetch-limited wave spectra*. Licentiate thesis in Geophysics. University of Helsinki. 75 pp.
- Kahma, K. K., 1981. On two-peaked wave spectra. *Finnish Mar. Res.*, **248**, 87–116.
- Kahma, K. K., J.-V. Björkqvist, M. M. Johansson, H. Jokinen, U. Leijala, J. Särkkä, K. Tikka and L. Tuomi, 2016. *Turvalliset rakentamiskorkeudet Helsingin rannoilla 2020, 2050 ja 2100*. 96. <http://www.hel.fi/static/kv/turvalliset-rakentamiskorkeudet.pdf>. City of Helsinki, Real Estate Department, Geotechnical Division.
- Kahma, K. K. and H. Pettersson, 1994. Wave growth in a narrow fetch geometry. *The Global Atmosphere and Ocean System.*, **2**, 253–263.
- Kahma, K. K., K. Tikka, L. Tuomi, H. Jokinen and H. Pettersson, 2022. *A statistical wave packet refraction model*. In preparation.
- Kahma, K. K., K. Tikka, L. Tuomi, H. Jokinen, H. Pettersson and A. Uttula, 2015. *Merkitsevän aallonkorkeuden puolen metrin rajan määrittäminen Suomen rannikolla*. Unpublished. Liikenteen turvallisuusvirasto, Liikennejärjestelmä/Tutkimus.
- Komen, G. J., L. Cavaleri, M. Donelan, K. Hasselmann, S. Hasselman and P. A. E. M. Janssen, 1994. *Dynamics and modelling of ocean waves*. Cambridge University Press.

- Pettersson, H., 2004. Wave growth in a narrow bay. *Finnish Institute of Marine Research, Contributions*, **9**. Ph.D thesis, University of Helsinki, Faculty of sciences, 1–33.
- Pettersson, H., K. K. Kahma and L. Tuomi, 2010. Wave Directions in a Narrow Bay. *J. Phys. Oceanogr.*, **40** (1), 155–169. DOI: 10.1175/2009JP04220.1.
- Tuomi, L., K. K. Kahma and H. Pettersson, 2011. Wave hindcast statistics in the seasonally ice-covered Baltic Sea. *Boreal Environment Research*, **16**, 451–472.
- Tuomi, L., H. Pettersson, C. Fortelius, K. Tikka, J.-V. Björkqvist and K. K. Kahma, 2014. Wave modelling in archipelago - sheltering, depth-induced wave breaking and refraction. *Coastal Engineering*, **83**, 205–220.
- van Vledder, G. Ph., 1990. Directional responses of wind waves to turning winds. *Communications on hydraulic and geotechnical engineering*, **90** (2). Doctoral thesis, Delft University of Technology, Faculty of Civil Engineering, 252 pp.